Thermal IR Radiation Sensing Using MEMS/NEMS

NICOLAS BEAUDOIN, MATHIS TURGEON-ROY, AND JOHNSON ZHANG

1. Introduction

Micro electromechanical systems (MEMS) and Nano electromechanical systems (NEMS) have proved to be an effective solution for high precision sensing of many phenomena. Their small size, their integrability with electronic circuits and their high responsivity have made them a common choice for precise measurement of pressure, acceleration, vibration and magnetic fields. This report presents MEMS and NEMS sensor as a solution for high precision infrared radiation sensing at room temperature, potentially filling a gap in performance that traditional sensors are not able to achieve.

2. Problem Statement

The current most widespread technology to detect radiation is the photodetector. The working principle of this technology is based on the interaction of a semiconducting material with the photon themselves. The process in which the radiation is detected has three key stages. First, the incident photons are absorbed by the semiconductor, generating excess electron hole pairs. Next, these charge carriers are transported across the absorption or transit region. Finally, the carriers are collected to produce a photocurrent.[1] This scheme enables photodetectors to achieve the ultimate fundamental detectivity limit of radiation sensing, which is a precision down to a single photon. Nonetheless, photodetectors have two major limitations.

To begin, thermionic emissions in the semiconductor produce what is commonly called dark current.[2] This dark current is the main source of noise in photodetectors and often dominates the signal at room temperature. The equation for thermionic emission current (also known as dark current) is

$$i_T = aAT^2 exp\left(-\frac{e\emptyset}{K_B T}\right) \quad (1)$$

Where i_T is the dark current, a is a constant equal to $1.2 \times 10^{-6} \frac{A}{m^2 K^2}$ for pure metals, A is the area of the cathode, $\emptyset$ is the work function and K_B is the Boltzmann constant. [2] The relationship clearly demonstrates the impact of the temperature on the magnitude of the dark current noise and the importance of cooling the cathode for the sensor to perform well. For this reason, photodetectors often require cryogenic cooling to achieve high precision sensing, which is expensive and inconvenient for implementation in most applications.

Secondly, radiation needs to carry enough energy to generate electron hole pairs in the semiconductor. The energy of a photon is directly proportional to the radiation frequency. Consequently, if the radiation's frequency is too low, it will not have enough energy to generate an electron hole pair, instead it will simply make the electrons vibrate, which constitute a radiative heat transfer. Figure 1 shows that the quantum efficiency (hole-pairs produced for every absorbed photon) for most common photodetector materials drops to almost 0 for wavelengths superior to 1 μm (frequency lower than 10^{15} Hz).

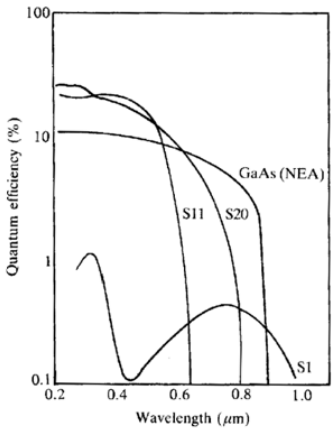

Figure 1 - Quantum efficiency as a function of the radiation wavelength for common photodetector materials [2]

The wavelength at which this drop occurs coincides with the beginning of the infrared (IR) spectrum region (700 nm to 1mm wavelength). For this reason, IR radiation sensing technologies tend to base their measure on the heat transferred rather than the photon absorption.

The most common thermal-based infrared sensors are resistive technologies. In the most basic form, they are composed of a thermistor, which is simply a semiconductor which has its conductivity varying with temperature, with a voltage applied on both ends. As the thermistor is exposed to radiation, its temperature increases because of radiative heat transfer and its conductivity changes. The current flowing through the thermistor is proportional to the conductivity and constitute the output signal of the sensor.[3] (See figure 2)

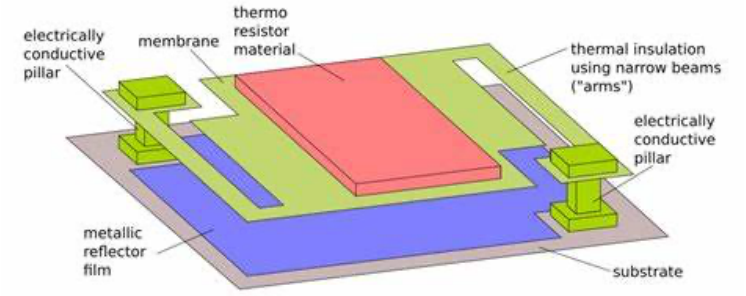

Figure 2 - Simplified representation of a micro bolometer (resistive thermal based IR sensor)[4]

However, unlike photodetectors with visible light, the detectivity of these technologies is still far away from the fundamental limit.[2] Nonetheless, recent research on a MEMS-based approach suggests new, unprecedented levels of precision could be achieved.

3. Physics Background

3.1 Fundamental Sensitivity Limit

The fundamental limit for thermal based sensing is the thermal fluctuation noise. This noise originates from the heat exchange of the sensor with its environment. It causes the temperature of the sensor itself to be unstable and consistently undergo some small fluctuations. [5] These

are unavoidable, and there are few ways they can be reduced with the sensor design. Therefore, if a thermal based sensor reaches the point where the thermal fluctuations become the limiting factor of its precision, it is as good as it can be.

The problem with resistive technologies is that they are most often limited by another source of noise called Johnson-Nyquist noise. This noise originates from the thermal agitation of electrons in the current that serves as output signal from the sensor. Electrical noise being proportional to the electrical resistivity, [3] resistive detectors face a challenging dilemma. On one hand, a good electrical conductor would reduce the Johnson-Nyquist noise, but on the other hand, responsivity of the sensor would suffer from a good thermal conductor.[5] The development of resistive sensors reaching the thermal fluctuation limit holds very low promise, as both conductivities are usually proportional through the Wiedemann-Franz law.[6] (See equation 2)

$$\frac{\kappa}{\sigma} = LT \qquad (2)$$

Where κ is the thermal conductivity, σ is the electrical conductivity, L is the Lorenz number equal to $2.44 \times 10^{-8} \frac{V^2}{K^2}$ and T is the temperature.

MEMS resonator sensors have the advantage of not being subject to electrical noise. Nevertheless, they are affected by two other important additive noise sources that are not considered for resistive sensor:

- Thermomechanical noise

Thermomechanical fluctuations are caused by the random motion of particles induced by their thermal energy. These fluctuations will interfere with the oscillation of the resonator even when at rest and bring uncertainty on the oscillation frequency. (See figure 3) Exact expression for thermomechanical noise differs with the geometry of the system. However, for all micro resonator sensors presented, the achievement of a high Q factor is a point of focus to reduce thermomechanical noise.

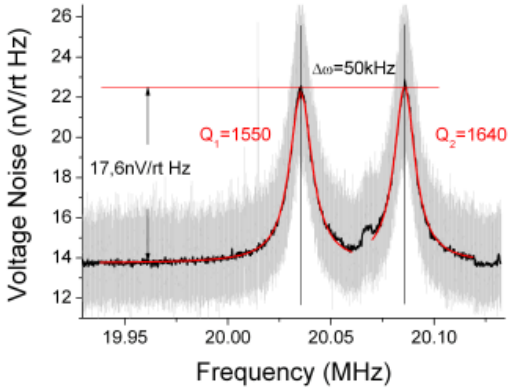

Figure *3* - Thermomechanical noise spectral density of a micro resonator [7]

- Detection read-out noise

An additional complexity with using micro resonator as a sensor is that the motion of the micro resonator being the brut output signal, a read-out scheme is necessary to detect the vibration and translate it in an electrical signal that computers can analyze. The read-out method also comes with its own set of noise sources that will ultimately impact the detectivity of the sensor. Detection read-out noise is highly dependent on the type of process employed to read out the oscillation. Read-out and actuation (usually related to the choice of read-out) for all different approaches will be discussed in their respective sections as well as the type of noises they add to the system.

3.2 IR Radiation's Effect on Resonance Frequency

The functioning of these novel sensors relies on a physical correlation between IR radiation and resonance frequency. This relation can be broken down in more direct relationships. Firstly, IR radiation has a heat transfer effect, as expressed by the Stephen-Boltzmann law

$$Q_R = \sigma \varepsilon A (T_{source}^4 - T_{sensor}^4) \quad (3)$$

where the radiative heat Q_R can be determined by the Stefan-Boltzmann constant σ, the emissivity ε, the area of the surface A, and temperatures T_{source} and T_{sensor}. As heat is absorbed by the sensor, the resonator's temperature increases leading to thermal expansion in the material. The linear elongation l can be determined by

$$l = \alpha \cdot \Delta T \quad (4)$$

where α is the linear expansion coefficient of the material for a temperature change ΔT. The dimensions of the sensor being fixed, this physical strain l is counteracted by an increase in stress σ_{stress}, according to the Young's modulus E of the membrane.

$$\sigma_{stress} = E \cdot l \quad (5)$$

The change in stress induced by the heat transfer affects the spring constant k of the vibrating membrane. The specific spring constant equation depends on the geometry of the resonating element, but in the case of a string trampoline, the spring behavior is determined by the equation for a stressed beam

$$k = \frac{4\,\sigma_{stress} A_c}{L} \quad (6)$$

where the A_c is the cross-sectional area and L the length of the string. The takeaway of this equation is that as the (tensile) stress increases, the spring constant also increases linearly. The spring constant becomes useful for determining the resonance frequency, as the system can effectively be represented by a mass-spring system. Since damping can be deemed negligible, we can assume that

$$\omega_n \cong \omega_r \quad (7)$$

for natural frequency ω_n and resonance frequency ω_r. Given that the natural frequency for a mass spring system is readily known, we may deduce that the resonance frequency is thus

$$\omega_r = \sqrt{\frac{k}{m}} \quad (8)$$

Since that the mass m remains constant, regardless of temperature, the spring constant is the only parameter of the resonance frequency, meaning that a parameterized link can be established between the latter, and the IR radiation. While this only a conceptual estimate, and that the true relationship depends on the specific geometry of the resonator as well as any source of noise, we may conclude that the analytical link between temperature change and frequency being

$$\omega_r = \sqrt{\frac{4\,E\,\alpha\,\Delta T\,A_c}{m\,L}} \quad (9)$$

For what is of the link between IR radiation and the change on temperature, this is partially dependent on the design of the sensor and would result from its own specific thermal modeling. However, once this relation is known the amount of IR radiation emitted, or even the temperature of the measured object T_{source} can be deduced.

2.3 Control Method

Although read-out of the oscillation of the resonator and actuation of the resonator are done differently for most presented cases, the control method principles are very similar and fundamental to the operation mode of micro resonator sensors.

A phased locked loop (PLL) scheme along with a lock-in amplifier is used to periodically compare the driving frequency with measured oscillating frequency. As the resonance frequency shifts due to radiative heating, the control loop employed a proportional, integrative, derivative (PID) controller to follow the resonance frequency shift. Which means that the control loop will always actuate the resonator to its resonance frequency. See figure 4 for a schematic representation of the control scheme represented for one of the sensors analyzed in this report:

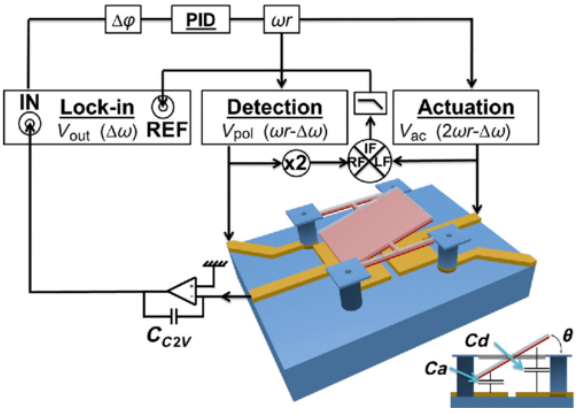

Figure 4 - Schematic of a NEMS resonator and its readout scheme [8]

4. Different Solution Approaches

4.1 Article 1 - 12-μm-Pitch Electromechanical Resonator for Thermal Sensing [8]

The electromechanical resonator is an uncooled IR detector that utilizes torsional resonator arrays. Each resonator consists of an H-shaped nanorod that is 9 μm long, and the plate that is 250×30 nm^2. The design is optimized for future integration in thermal imaging system.

Actuation, and results of the torsional movement measurements are obtained through capacitance output. Theoretical noise equivalent power (NEP) for this read-out method is given by:

$$NEP_{elec} = \frac{1}{R_f}\frac{1}{2Q}\frac{\sqrt{\langle V_n^2 \rangle}}{V_{out}} \tag{10}$$

Where NEP_{elec} is the noise equivalent power associated with the electronic readout scheme, R_f is the thermal response, Q is the quality factor, V_n is the voltage fluctuation and V_{out} is the voltage at the detection output electrode.

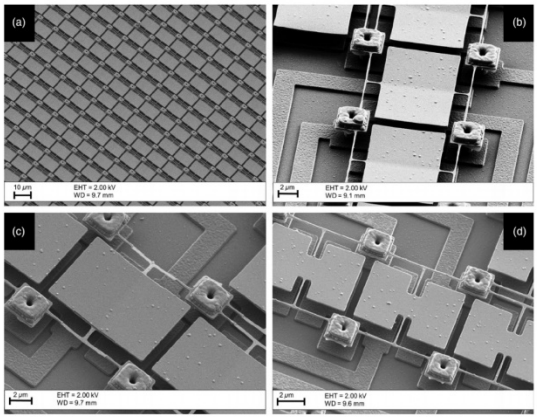

Figure 5 - SEM images of the torsional resonator array [8]

4.2 Article 2 - Heat Transport in Silicon Nitride Drum Resonators and Its Influence on Thermal Fluctuation – Induced Frequency Noise [9]

As the premise behind the infrared imaging is the measurement of radiation and conduction in heat transport, one of the main goals to improve the existing technology is to increase the thermal response time of silicon nitride membranes and to approach the fundamental limit as near as possible. For larger silicon nitride membrane areas, thermal fluctuations can be greater than thermomechanical contributions to frequency noise, when other noise sources are considered. Often time, it is the thermal fluctuation noise itself that dominates the inherent frequency noise in the silicon nitride membrane.

Silicon nitride square membrane drum resonator is used as infrared radiation sensor. Membrane's thickness is 100 nm and side length from 1 mm to 12 mm were tested. The oscillation was read out using an optical interferometer and the membrane was actuated at resonance frequency with a piezo element (see figure 10). Optical measurement seems to be the best approach amongst the ones evaluated in this report as the article does not cite any problematic or questioning regarding the read-out system unlike electrostatic and magnetomotive scheme. Read noise for this method can be evaluated as:

$$S_y = \left(\frac{1}{2Q}\frac{Sx}{A_{rss}}\right)^2 \tag{11}$$

Where S_y is the readout noise, Q is the quality factor, Sx is the amplitude noise of the interferometer, and A_{rss} is the drive amplitude.[10]

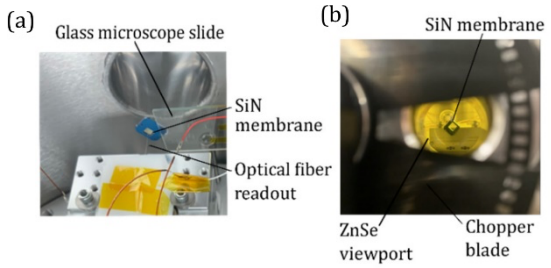

Figure 6 - Close up image of the SiN resonator [9]

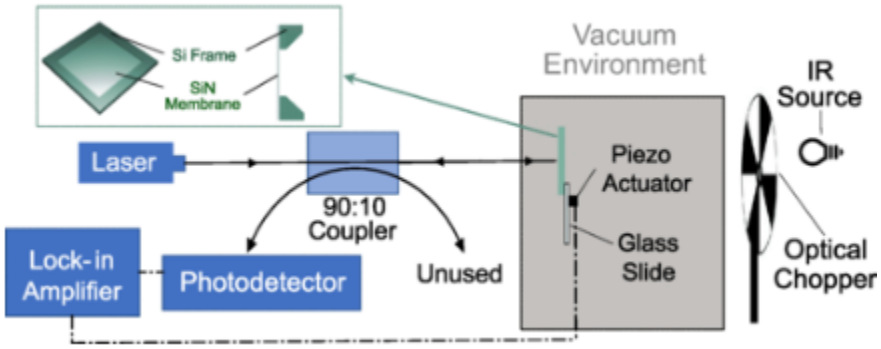

Figure 7 - Readout scheme of micro resonator sensor [9]

4.3 Article 3 - Shape Memory Polymer Resonators as Highly Sensitive Uncooled Infrared Detectors [11]

Shape memory polymer (SMP) discs with 520 µm radius and 10 µm thickness is used as micro resonators. SMP was chosen here because the young modulus of the material is highly dependent on temperature. Transition between the rigid rubbery state of the material makes the resonance frequency shift greater per temperature variation than a similar resonator made of silicon nitride for example. However, this gain in temperature coefficient of the resonance frequency also comes with the inconvenient that SMP has a much lower intrinsic quality factor compared to material like silicon nitride. Therefore, silicon nitride membranes are used to achieve high Q quality factors, as substrates for the shape memory polymers. A two orders of magnitude improvement of temperature coefficients of frequency is claimed in the article.

Actuation of the resonator is done through piezoelectric element and oscillation read out with an optical interferometer. Therefore, noise associated with read-out is very similar to the one presented above and will not be presented again.

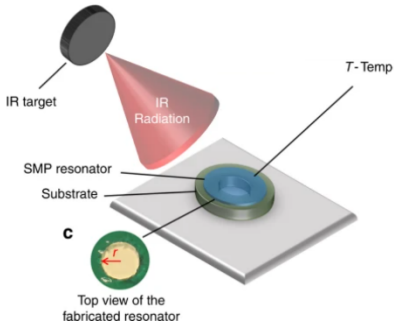

Figure 8 - SMP resonant sensor schematic [11]

4.4 Article 4 - Thermal IR Detection with Nanoelectromechanical Silicon Nitride Trampoline Resonators [12]

The membrane acts as a trampoline, when blasted with photons, its resulting resonance frequency shift is measured. A few different resonator types are used in this study, detection area ranging from 45 × 45 µm to 455 × 455 µm, as well as a complete drum without tethers at 1000 × 1000 µm. The experiment starts off with a thermal IR light source with a range from 1 to 25 µm, a PID controller is used to maintain a constant detector temperature at 20°C.

State of the art uncooled thermal detectors' sensitivity are still several orders of magnitude below the fundamental detection limit, caused by the power fluctuations of thermal radiation from the detector and its background. Low energy IR photons are absorbed and resulted heating is measured; during the measurement process, it can be electronically influenced by noise. While it is not feasible to completely remove such effects produced by noise, the goal is to minimize it, by using drum resonators noise equivalent power can be improved, its influence lowered to a minimum (Table 1). Drum resonators made of silicon nitride also have a distinctive property, that it can reach an intrinsic sensitivity in the fW-regime. Notably, the thermal response time can also be improved by a factor of 3. The author speculates that this design will have the potential to reach the ultimate photon noise sensitivity limit.

Readout of this sensor is based on a magnetomotive transduction scheme. The magnetic field employed is created by 2 permanent magnets, producing a field strength of 0.6 T. As the gold traces move in the magnetic field, they produce an induction voltage amplified by a differential low-noise voltage preamplifier. Actuation of the membrane works with the reversed principle. The expression of NEP for the readout noise of this sensor is unfortunately not presented by the author.

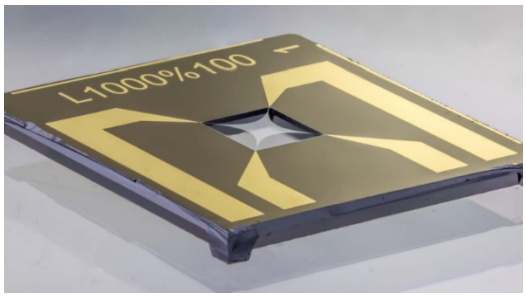

Figure 9 - SiN Trampoline Resonator Schematic [12]

4.5 Fabrication Technique and Process of Silicon Nitride Trampoline Resonators [12]

1. A fresh plain wafer is prepared and applied with double sided silicon nitride layers.
    1.1. Low-stress silicon-rich silicon nitride thin film acts as the membrane, it is 50 nm thick and deposited through chemical vapor deposition.
    1.2. Trampoline tethers measure 5 µm wide.
    1.3. Each silicon frame measures 380 µm thick.
    1.4. Each chip measures 5 by 5 mm, and frame size of 1 by 1 mm.
2. Photoresist is then spin-coated on the top layer.
3. Photolithography is applied on the photoresist creating the cutout structure for the gold electrodes.
4. Gold traces are deposited through thermal evaporation, occupying the spaces between photoresist and a layer on top.
5. Excess gold and photoresist are removed by a lift-off process.
    5.1. Gold electrodes measure 1 µm wide, with a thickness of 190 nm.
    5.2. Beneath the electrodes is a layer of 10 nm chromium adhesion applied through thermal evaporation.
6. Photoresist is then spin-coated on the top and the bottom layers.
7. Reactive ion etching is applied on the top layer, structuring the top photoresist layer.
8. Reactive ion etching is applied similarly on the top layer, structuring the layer of silicon nitride beneath the photoresist which was removed in step 7.
9. A square window is used to patterned on the bottom photoresist, exposing the silicon nitride on the bottom layer, top layer is removed similarly through patterning.
10. Reactive ion etching is applied on the bottom layer, removing the silicon nitride exposed in step 9.
11. Silicon is etched by potassium hydroxide; silicon nitride trampoline is released.
12. Platinum film is deposited via thermal evaporation on the bottom side, providing an impedance-matched absorber.
    12.1. Providing a flat spectral response for wavelengths between 1 to 25 µm.
    12.2. 50% optimal absorption over the spectral range, measured by Fourier-transform IR spectroscopy.

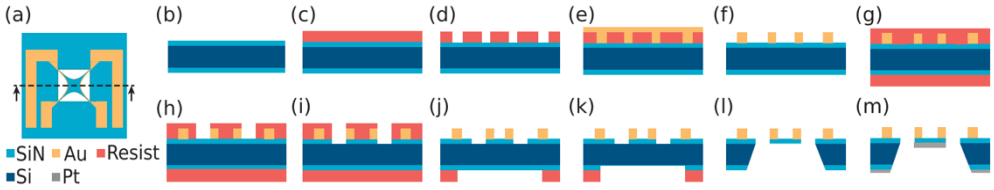

Figure 10 – Sample fabrication process of SiN trampoline resonator with gold traces [12]

5. Approach Evaluation

While comparing the prospects of each approach is a difficult task, as all four are currently in development, a preliminary evaluation of performance can enable a decision as to which approach is the most promising. Given to limited information and numerical results of each paper, performance comparison is not straightforward. Noise Equivalent Temperature Difference (NETD) could be the ideal comparison metric, but this value is not available for two of the four papers. Using a combination of Q factor and Noise Equivalent Power (NEP), one can generally rank the overall performance of sensors, despite the missing values.

Table 1 Comparison of Key Performance Metrics [8,9,11,12]

	Article 1	Article 2	Article 3	Article 4
Frequency Shift [Hz]	21	9	15	8
Maximum Q factor	900 – 3000 Main 1800	1×10^6	1×10^5	Not Stated
Noise Equivalent Temperature Difference (NETD) [K]	0.18	Not Stated	0.022	Not Stated
Thermal Response Time [ms]	0.5	30	200 - 400	4
Noise Equivalent Power (NEP) [pW/√ Hz]	< 20	41	Not Stated	7
Allan Deviation at Room Temperature	3×10^{-7}	1×10^{-8}	1×10^{-5}	1×10^{-6}
Thermal Conductance (G) [W/K]	5×10^{-8}	NA	Requested from Author	NA

Examining Q factor, Article 2 appears to have maximized this value, but it is unclear how it ranks relative to Article 4. Looking at NEP, Article 4 seemed to minimize this value best, with missing values for Article 3. Ultimately this means that either the approach from Article 2 or Article 4 could be deemed the most promising, depending on the importance attributed to Q factor relative to NEP. Since NEP is a more direct measure of noise, and hence the sensors precision, it was deemed a more valuable metric for this analysis, even though high Q factor could eventually lead to more promising results with more development.

Since Article 4 has lowest NEP, with Article 3 being an unlikely contender due to its Q factor positioning, one can come to the preliminary conclusion that the trampoline resonator with magnetomotive read-out approach presented in Article 4 could be deemed as the most promising solution.

Other takeaways from comparing the results of each article did establish some general conclusions. For one, the trampoline/membrane format seemed to offer the best performance compared to other designs, offering better responsiveness and precision. On the other hand, the limited manufacturing capability tested for the capacitive measurement approach offered poor precision due to parasitic capacitance read-out, which may indicate other difficulties in reducing noise. Piezoelectric actuation offered the most elegant solution, but optical measurement may not be sufficiently compact to be applicable in general use. All in all, even though the magnetomotive approach of Article 4 appears to lead the pack, other approaches, or even a combination of different technologies, may offer the best performing solution in the end.

References

[1]
P. Basu, “Photodetector Fundamentals,” in *Handbook of Optoelectronic Device Modeling and Simulation*, CRC Press, 2017.
[2]
R. Taylor, “Teaching Material.” Accessed: Nov. 06, 2024. [Online]. Available: https://users.physics.ox.ac.uk/~rtaylor/teaching.shtml
[3]
P. W. Kruse, “Can the 300-K radiating background noise limit be attained by uncooled thermal imagers?,” in *Infrared Technology and Applications XXX*, SPIE, Aug. 2004, pp. 437–446. doi: 10.1117/12.539388.
[4]
“Microbolometer,” *Wikipedia*. Nov. 16, 2024. Accessed: Nov. 18, 2024. [Online]. Available: https://en.wikipedia.org/w/index.php?title=Microbolometer&oldid=1257683689
[5]
R. St-Gelais, “Demonstration of frequency stability limited by thermal fluctuation noise in silicon nitride nanomechanical resonators,” *Applied Physics Letters*, vol. 122, no. 19, p. 193501, May 2023, doi: 10.1063/5.0145780.
[6]
G. V. Chester and A. Thellung, “The Law of Wiedemann and Franz,” *Proc. Phys. Soc.*, vol. 77, no. 5, p. 1005, May 1961, doi: 10.1088/0370-132[1]
M. Piller, J. Hiesberger, E. Wistrela, P. Martini, N. Luhmann, and S. Schmid, “Thermal IR Detection With Nanoelectromechanical Silicon Nitride Trampoline Resonators,” IEEE Sensors Journal, vol. 23, no. 2, pp. 1066–1071, Jan. 2023, doi: 10.1109/JSEN.2022.3223439.
8/77/5/309.
[7]
E. Mile, “Systèmes électromécaniques nanométriques a base de nano-fils de silicium et nanotubes de carbone,” phdthesis, Ecole Polytechnique X, 2010. Accessed: Nov. 18, 2024. [Online]. Available: https://pastel.hal.science/pastel-00551920
[8]
L. Laurent, J.-J. Yon, J.-S. Moulet, M. Roukes, and L. Duraffourg, “$12\text{\ensuremath{-}}\ensuremath{\mu}\mathrm{m}$-Pitch Electromechanical Resonator for Thermal Sensing,” *Phys. Rev. Appl.*, vol. 9, no. 2, p. 024016, Feb. 2018, doi: 10.1103/PhysRevApplied.9.024016.
[9]
N. Snell, “Heat Transport in Silicon Nitride Drum Resonators and its Influence on Thermal Fluctuation-Induced Frequency Noise,” *Phys. Rev. Appl.*, vol. 17, no. 4, 2022, doi: 10.1103/PhysRevApplied.17.044019.
[10]
S. Schmid, L. G. Villanueva, and M. L. Roukes, Fundamentals of Nanomechanical Resonators. Cham: Springer International Publishing, 2023. doi: 10.1007/978-3-031-29628-4.
[11]
U. Adiyan, T. Larsen, J. J. Zárate, L. G. Villanueva, and H. Shea, “Shape memory polymer resonators as highly sensitive uncooled infrared detectors,” *Nat Commun*, vol. 10, no. 1, p. 4518, Oct. 2019, doi: 10.1038/s41467-019-12550-6.
[12]
M. Piller, J. Hiesberger, E. Wistrela, P. Martini, N. Luhmann, and S. Schmid, “Thermal IR Detection With Nanoelectromechanical Silicon Nitride Trampoline Resonators,” *IEEE Sensors Journal*, vol. 23, no. 2, pp. 1066–1071, Jan. 2023, doi: 10.1109/JSEN.2022.3223439.